Armenian Journal of Physics, 2010, vol. 3, issue 1, pp. 34–45

OPTICAL CLOCK, RADIO FREQUENCY TIMING TECHNIQUE AND A NEW EARTH-BOUNDED GRAVITATIONAL RED-SHIFT EXPERIMENT

Amur Margaryan

A. I. Alikhanian Yerevan Physics Institute, Yerevan, Armenia
Received January 20, 2010

Abstract – The merging of continuous wave laser-based precision optical-frequency metrology with mode-locked ultrafast lasers has led to precision control of the visible frequency spectrum produced by mode-locked lasers. Such a phase-controlled mode-locked laser forms the foundation of an optical clock or "femtosecond optical frequency comb (OFC) generator," with a regular comb of sharp lines with well-defined frequencies. Combination of OFC with a radio frequency timing technique results in a new tool for precision time or frequency measurements. A new, Earth-bounded gravitational red-shift precise experiment is discussed.

Key words: optical clock, optical frequency comb, optoelectronic heterodyne, gravitational red-shift

1. Introduction

All clocks consist of two major components: some device that produces periodic events or "clock ticks," and some means for counting, accumulating, and displaying each tick. For example, the swing of a pendulum provides the periodic events that are counted, accumulated, and displayed by means of a set of gears driving a pair of clock hands.

If the frequency of the oscillator is locked to the atomic transition frequency, then the time generated can have improved long-term stability and accuracy. For an atomic clock based on a microwave transition, high-speed electronics count and accumulate a defined number of cycles of the reference oscillator to mark a second of time. The basic concepts are the same for an atomic clock based on an optical transition at a much higher frequency.

The recent development of ultrabroad femtosecond optical frequency comb (OFC) based on mode-locked lasers has provided a relatively simple and straightforward way to translate optical frequency standards to other optical and microwave frequencies [1, 2]. The Fourier transform of a femtosecond pulse train is a comb of evenly spaced frequencies, typically spanning some 10% of the optical range. The frequency of individual femtosecond comb teeth, f_n, can be uniquely described by the relation $f_n = n \times f_r + f_0$, where n is a large integer (~ 500,000), f_r is the repetition rate of the laser, and f_0 is the offset of the entire comb from harmonics of f_r. Controlling two degrees of freedom of the comb precisely determines the frequency of each comb tooth f_n. Both f_r and f_0 are microwave frequencies, whereas the comb teeth f_n are optical frequencies; therefore the femtosecond OFC architecture provides a phase-coherent translation between the two frequency ranges.

There are different schemes possible to achieve stabilization of the comb, each allowing examination of different quantities. One specific use of the femtosecond comb synthesizer is that of a microwave synthesizer. In this case, the comb is stabilized to an optical oscillator and the microwave output of the comb appears as the repetition rate of the laser. The quality of the stabilized optical pulse trains can be evaluated with the basic apparatus based on two different approaches. The first approach is an optical cross-correlation technique; the second one is a classic heterodyning of two RF frequencies synthesized by using fast photodiodes. It was demonstrated that the fractional frequency instability of the OFC microwave synthesizer is $2\times10^{-14}/\tau$, and could be improved by at least a factor of 10 upon elimination of excess photodetection noise [3].

We are proposing a new heterodyning approach for OFCs, based on a radio frequency (RF) timing technique. In this approach the microwave output from the RF synthesizer, generated by one of two OFCs, is used for driving the RF phototube [4] or streak camera [5], which detects simultaneously both OFCs. The proposed new method allows avoiding of excess photodetection noise [3] and internal drift of the tube [5] and achieves the 10^{-18} accuracy level.

As clocks are fundamental tools for confirming and testing the present description of physical phenomena encoded in the Standard Model and in Einstein's special and general theory of relativity [6], the proposed method opens new possibilities for precise clock experiments. The dedicated experiment for precise measuring of the gravitation red-shift will be discussed briefly.

2. The RF timing technique

2.1. Principles of operation

The operational principles of the technique are described in [4] (and references therein) and the schematic layout of the RF phototube or streak camera is shown in Fig. 1.

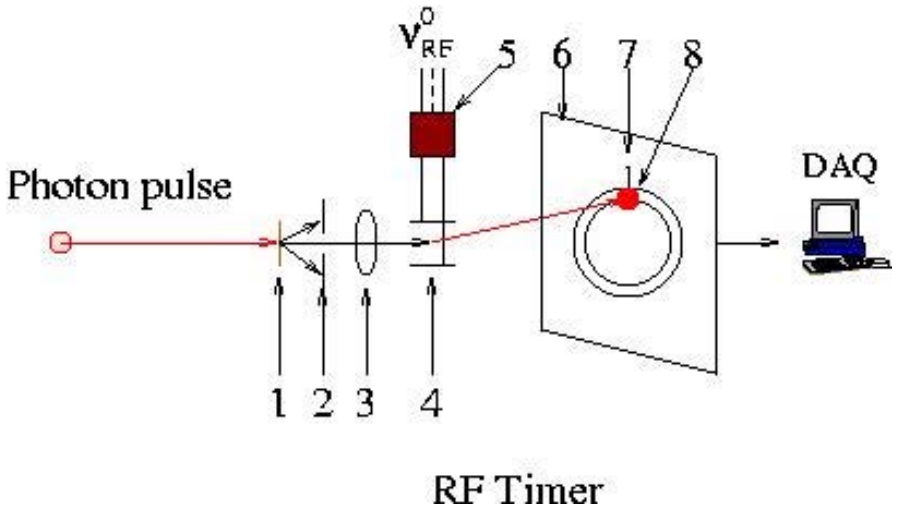

Fig. 1. Schematic layout of the RF phototube. 1 – photo-cathode, 2 – electron transparent electrode, 3 – electrostatic lens, 4 – RF deflector, 5 – $\lambda/4$ coaxial RF cavity, 6 – SE detector, 7 – arbitrary reference, 8 – image of photo-electrons.

The primary photon pulse hits the photocathode (1) and produces photo-electrons (PEs). These electrons are accelerated by a voltage V applied between the photocathode and an electron transparent electrode (2). Due to this the time spread of electrons is minimized. The electrostatic lens (3) then focuses and transposes the electrons isochronously onto the screen (7) at the far end of the tube, where the secondary electron (SE) detector is placed. The time structure of the produced PE bunch is identical to that of the light pulse. Along the way the electrons are passed through the circular sweep RF deflection system (4). They are deflected and form a circle on the screen of the detector, where the time structure of the input photon signal is transferred into spatial PE image (8) on a circle, calibrated in time by the sweep itself, and detected. The detection of the RF analyzed PEs is accomplished with a position sensitive detector. In this way the RF phototube transposes the linear time axis into a circle one. The corresponding phases of the applied RF field then are fixed, detected and stored. Meanwhile in such a detection system the timing error sources are minimized, because PE's are timed before the necessary further signal amplification and processing. Practically, the RF deflection system operates as a high frequency oscilloscope and times PEs before the electron multiplication process starts in the detector. The electron multiplication process in this case is used to determine the position on the scanning circle.

2.2. Stand-alone operation: random photon source

The time or phase instabilities of the RF timing technique are conditioned by instabilities of the RF oscillator and phototube.

The signal V_{RF} delivered by an RF oscillator can be written [7]

$$V_{RF}(t) = V_{RF}^0 \sin[2\pi\nu_{RF}^0 t + \phi_{RF}(t) + \phi_{RF}^0],$$

where we have assumed that the amplitude V_{RF}^0 is constant. The quantity ν_{RF}^0 is the constant nominal frequency and referred to the definition of the second, and t is the ideal proper time. The phase $\phi_{RF}(t)$ contains the deviations, both random and systematic, relative to the ideal periodic variations, ν_{RF}^0. The quantity ϕ_{RF}^0 represents the nominal phase.

The instantaneous frequency $\nu_{RF}(t)$ is defined by

$$\nu_{RF}(t) = \nu_{RF}^0 + \frac{1}{2\pi}\frac{d\phi_{RF}(t)}{dt}.$$

The relative frequency offset of the oscillator is given by

$$y_{RF}(t) = \frac{\nu_{RF}(t)}{\nu_{RF}^0} - 1.$$

It represents as a relative value the instantaneous departure of the oscillating frequency from its minimal value.

The clock reading is incremented by the nominal value $1/\nu_{RF}^0$ of the period every time the total phase $2\pi\nu_{RF}^0 t + \phi_{RF}(t) + \phi_{RF}^0$ increases by 2π. The time indicated since the time origin is therefore

$$t_{RF} = t + x_{RF}(t),$$

where we have set

$$x_{RF}(t) = \frac{\phi_{RF}(t)}{2\pi\nu_{RF}^0}.$$

The quantity t_{RF} is the proper time of the RF oscillator. The proper time deviation resulting from imperfection in the oscillator is thus equal to $x_{RF}(t)$. This is the time instability of the clock with respect to an ideal reference time scale.

From the above definition, it is easy to show that

$$y(t) = \frac{dx(t)}{dt},$$

where $y(t)$ represents the relative frequency offset of an oscillator or a clock as a function of t and $x(t)$ its proper time deviation.

The photoelectron passes through the RF deflector at the time moment t^i and fixes the total phase of the RF oscillator:

$$\Phi_{RF}^i = 2\pi\nu_{RF}^0 t^i + \phi(t^i) + \phi_{RF}^0 = 2\pi\nu_{RF}^0 t^i + \phi_{RF}(t^i) + \phi_T(t^i) + \phi_{RF}^0$$

somewhere on the scanning circle. Here ϕ_{RF}^0 is a nominal phase, which is a constant for the given configuration of the experimental setup. For the arbitrarily calibrated position sensitive detector, for which the nominal phase ϕ_{RF}^0 on the scanning circle is selected arbitrarily, the time moment t^i is transposed to total phase Φ_{RF}^i; here the phase $\phi(t^i) = \phi_{RF}(t^i) + \phi_T(t^i)$ contains random and systematic deviations relative to the ideal periodic variations, due to the RF oscillator and phototube, respectively. The time moment t^{i+1} for the next photoelectron will be transposed to

$$\Phi_{RF}^{i+1} = 2\pi\nu_{RF}^0 t^{i+1} + \phi_{RF}(t^{i+1}) + \phi_T(t^{i+1}) + \phi_{RF}^0.$$

The time duration $\Delta t_{RF} = t^{i+1} - t^i$ is measured through total phase differences

$$\Delta\Phi_{RF} = \Phi_{RF}^{i+1} - \Phi_{RF}^i = 2\pi\nu_{RF}^0 (t^{i+1} - t^i) + \Delta\phi_{RF} + \Delta\phi_T,$$

where $\Delta\phi_{RF} = \phi_{RF}(t^{i+1}) - \phi_{RF}(t^i)$, $\Delta\phi_T = \phi_T(t^{i+1}) - \phi_T(t^i)$, and ν_{RF}^0 is the nominal frequency of the RF oscillator. In this way the absolute value of the duration of two photoelectrons $t^{i+1} - t^i$ is expressed through the value of ν_{RF}^0, with the random and systematic deviations relative to the ideal period equal to $\Delta x_{RF} + \Delta x_T$, where $\Delta x_{RF} = \Delta\phi_{RF} / 2\pi\nu_{RF}^0$, and $\Delta x_T = \Delta\phi_T / 2\pi\nu_{RF}^0$.

The CW photon beam produces a CW photoelectron flux, which forms a circle on the screen. The scanning speed of the PEs on the detector is $\upsilon = 2\pi R / T = 2\pi\nu_{RF}^0$. Here $T = 1/\nu_{RF}^0$ is the period of the RF field and R is the radius of the circle on the detector. For example, if $T = 2\times10^{-9}$ s ($\nu_{RF}^0 = 500$ MHz) and $R = 2$ cm, we have $\upsilon \geq 0.5\times10^{10}$ cm/s.

The short photon pulse produces a short photoelectron pulse, which forms a spot somewhere on the scanning circle depending on the phase of the applied RF field. By measuring coordinates of the spot, the phase of the RF field and consequently the time can be determined. The technical (or reading) time resolution by definition is $\Delta\tau_d = d / \upsilon$, where d is the size of the electron beam spot or the position resolution of the SE detector (if the electron spot is smaller). The time resolution $\Delta\tau_d$ is ≤ 20 ps, rms for a single photoelectron with $d = 1.0$ mm, $\nu_{RF}^0 = 500$ MHz and $R = 2$ cm.

In case of RF phototube [4], position of the photoelectrons on the circle can be determined by, e.g., using a direct readout scheme such as an array of small (~ 1 mm^2) pixels with one readout channel per pixel. In this case the RF phototube operates as a 50 GHz sampling optoscope and can be used as an optical waveform digitization device in the nanosecond and subnanosecond domain with ~2 ps internal timing resolution. In case of streak camera, position of the photoelectrons on the circle can be determined by, e.g., using readout system based on CCD.

2.3. Stand-alone operation: periodic photon source

Suppose the incident photon beam is an ideal OFC with a nominal photon pulse frequency $\nu_{ph}^0 = 1/T_{ph}$ (see Fig.2). The RF phototube driven signal with frequency ν_{RF}^0 can be expressed as

$$V_{RF}(t) = V_{RF}^0 \sin[2\pi\nu_{RF}^0 t + \phi_{RF}(t) + \phi_{RF}^0].$$

In such a case the RF phototube operates like a heterodyne for frequencies of the RF and OFC signals. The total phase of the heterodyned signal is:

$$\Phi_H(t) = 2\pi(\nu_{RF}^0 - \nu_{ph}^0)t + \phi_H^0 + \Delta\phi_{RF}(t) + \Delta\phi_T(t).$$

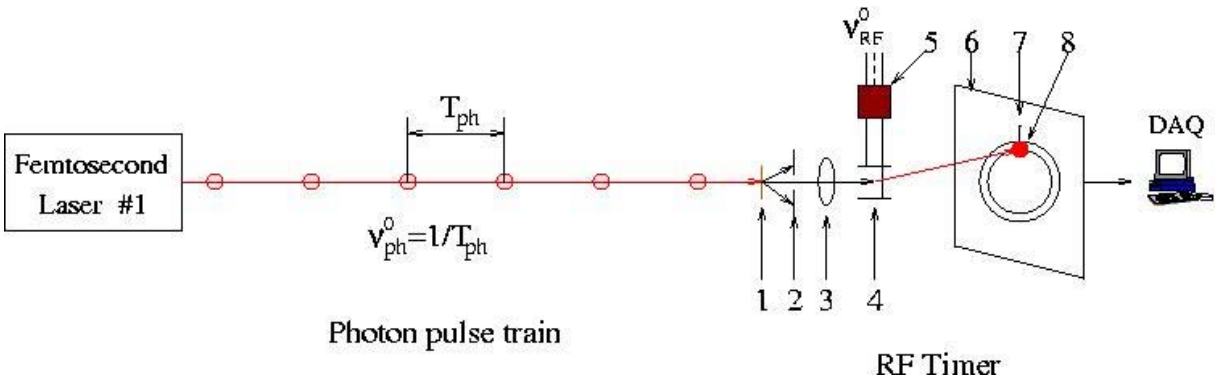

Fig. 2. Schematic layout of the RF phototube with periodic photon source. 1 – photo-cathode, 2 – electron transparent electrode, 3 – electrostatic lens, 4 – RF deflector, 5 – $\lambda/4$ coaxial RF cavity, 6 – SE detector, 7 – arbitrary reference, 8 – image of PEs.

The PE beam spot will drift on the scanning circle with speed $\upsilon = 2\pi R(\nu_{RF}^0 - \nu_{ph}^0)$, where R is the radius of the circle. The drift is clockwise for $\nu_{RF}^0 > \nu_{ph}^0$ and counterclockwise for $\nu_{RF}^0 < \nu_{ph}^0$. This feature can be used for precise comparison of two close frequencies, operational frequency of the RF deflector, ν_{RF}^0, with the photon pulse train frequency ν_{ph}^0. Continuous wave operation of the OFC and the RF phototube is the essential requirement for such a heterodyning system. The amplitude V_H^0 is determined by the RF phototube readout system. For time instability of the heterodyned signal we have:

$$\Delta x_H(t) = (1/2\pi\nu_H)\Delta\phi_H(t),$$

where $\nu_H = \left|\nu_{RF}^0 - \nu_{ph}^0\right|$ and $\Delta\phi_H(t) = \Delta\phi_{RF}(t) + \Delta\phi_T(t)$.

The case when $\nu_{RF}^0 = \nu_{ph}^0$ is known as a synchroscan mode and ideally with no system drift, i.e. when $\Delta x_H(t) = 0$, the position of the PEs spot should stay stable on the scanning circle. In reality, with stable OFC, the time instability of the heterodyned signal is determined by instabilities of the RF oscillator and the RF phototube. For precision measurements one needs to minimize these ingredients or operate the tube in a synchroscan mode with a reference femtosecond photon train.

2.4 RF phototube in synchroscan mode

Figure 3 shows a schematic diagram of a standard synchroscan mode of an RF phototube or streak camera.

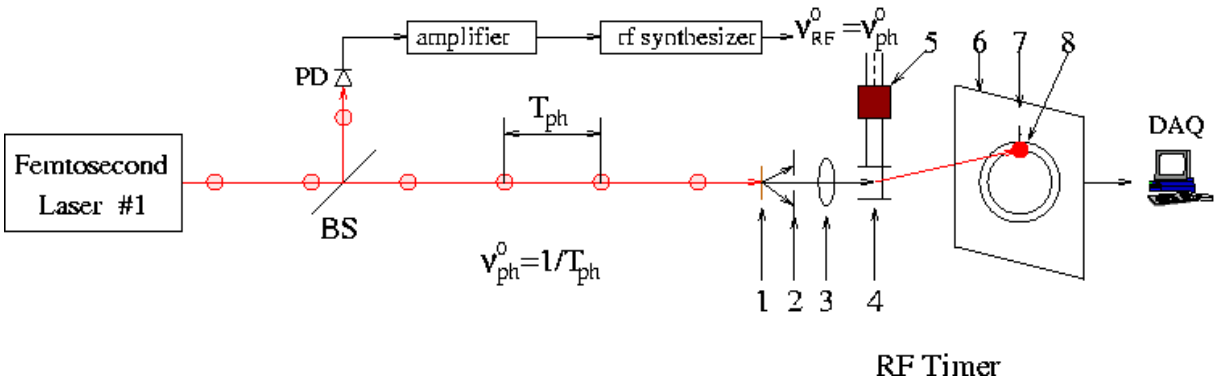

Fig. 3. Schematic diagram of the experiment with RF phototube in the synchroscan mode. BS – beam splitter, PD – photo diode, 1 – photocathode, 2 – accelerating electrode, 3 – electrostatic lens, 4 – deflection electrode, 5 – quarter wavelength coaxial cavity, 6 – position sensitive secondary electron detector, 7 – arbitrary reference fixed on SE detector readout system, 8 – SEs from reference beam.

The incident photon pulse train with a repetition rate ν_{ph}^0 is split in two parts. The first one is directed to the photodiode and RF synthesizer, which generates a sinusoidal signal $V_{RF}(t)$ synchronous to the femtosecond photon train for driven of the RF phototube or streak camera. This signal can be expressed as

$$V_{RF}(t) = V_{RF}^{0} \sin[2\pi\nu_{ph}^{0} t + \phi_{RF}(t) + \phi_{RF}^{0}].$$

The second part of the photon beam illuminates the photocathode. The resulting photoelectrons are extracted, accelerated, focused, deflected by an RF deflector and detected with a total phase

$$\Phi_{REF}(t) = \phi_{REF}(t) + \phi_{REF}^{0} = \phi_{RF}(t) + \phi_{T}(t) + \phi_{REF}^{0},$$

relative to an arbitrary fixed reference (7) on the position sensitive detector, and can be used as reference point (see later). The random and systematic deviations due to the RF synthesizer and phototube are equal to $\Delta x_{REF} = \Delta\phi_{REF} / 2\pi\nu_{ph}^{0}$. For the ideal tube and RF synthesizer, $\Delta x_{RF} = 0$, i.e. the position of photoelectrons on the scanning circle stay constant.

The temporal resolution of the technique is so high that every small component of instability in the RF synthesizer and phototube produces a noticeable drift. The instability of the OFC RF synthesizer is about or less than $2\times10^{-14}/\tau$ [3]. The instability of streak cameras has been investigated in [5]. A measure of instability of two streak cameras at the same time and in the same conditions (by using the same synchroscan signal) shows that each camera has its own intrinsic and stochastic drift. The measured drift is linear against time and amounts of about 8 ps in 15 min (or less than 10 fs in 1 s) for the both streak cameras. Therefore, systematic error of relative time measurements performed by streak camera in short (< 1 s) term is less than 10 fs. In the case of long term measurements, systematic deviations due to $\phi_{RF}(t)$ and $\phi_{T}(t)$ can be avoided by using the incident photon beam as a reference. This method is schematically shown in Fig. 4.

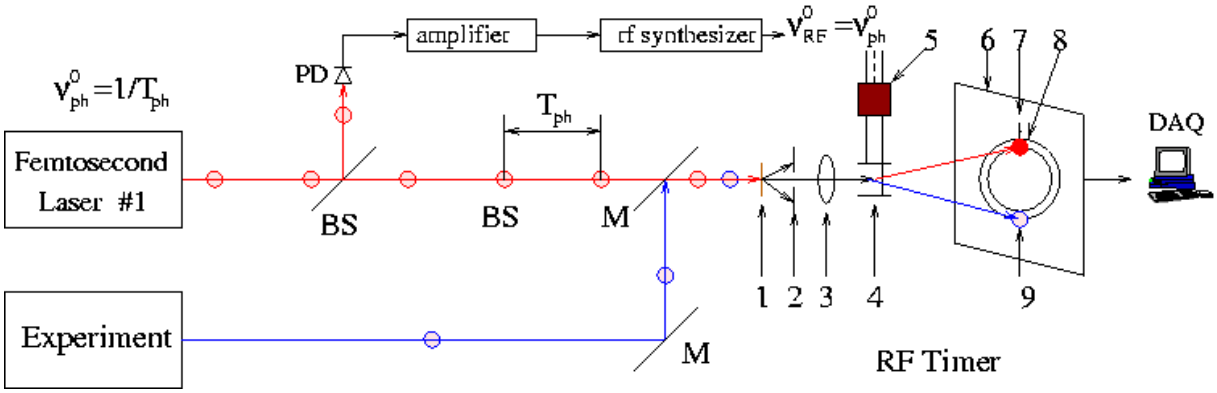

Fig. 4. Schematic diagram of the experiment with reference beam. BS – beam splitter, M – reflector, PD – photo diode, 1 – photocathode, 2 – accelerating electrode, 3 – electrostatic lens, 4 – deflection electrode, 5 – quarter wavelength coaxial cavity, 6 – position sensitive secondary electron detector, 7 – arbitrary reference fixed on SE detector readout system, 8 – SEs from reference beam, 9 – SEs from experiment.

In this case the light pulses of the experimental investigations are also directed to the photocathode and detected simultaneously with the reference photon beam. If the position of PEs from the experiment (9) is determined relative to the position of PEs from reference beam (8)

continuously, the long term drifts related to the RF synthesizer and phototube can be excluded. By this way 200 fs stability for hours has been achieved for streak cameras [5].

3. Optoelectronic heterodyne

The synchroscan mode of the RF phototube can be used for precision comparison of the frequencies of two OFCs. Figure 5 shows a schematic diagram of the proposed method which we call an optoelectronic heterodyne. The photon beam from the #1 OFC with a repetition rate ν_1^0 is split in two parts. The first part is directed to the photodiode and RF synthesizer, which generates a sinusoidal signal $V_{RF}(t)$ synchronous to the #1 photon train for driving the RF phototube. This signal can be expressed as

$$V_{RF}(t) = V_{RF}^0 \sin[2\pi\nu_1^0 t + \phi_{RF}(t) + \phi_{RF}^0].$$

The second part of the photon beam illuminates the photocathode. The resulting photoelectrons are extracted, accelerated, focused, deflected by an RF deflector and detected on the scanning circle with a total phase

$$\Phi_1(t) = \phi_1(t) + \phi_{1RF}^0 = \phi_{1RF}(t) + \phi_{1T}(t) + \phi_{1RF}^0.$$

The photoelectrons from the #2 OFC photon beam detected by the above system will have a total phase

$$\Phi_2(t) = 2\pi(\nu_1^0 - \nu_2^0)t + \phi_2(t) + \phi_{2RF}^0 = 2\pi(\nu_1^0 - \nu_2^0)t + \phi_{2RF}(t) + \phi_{2T}(t) + \phi_{2RF}^0.$$

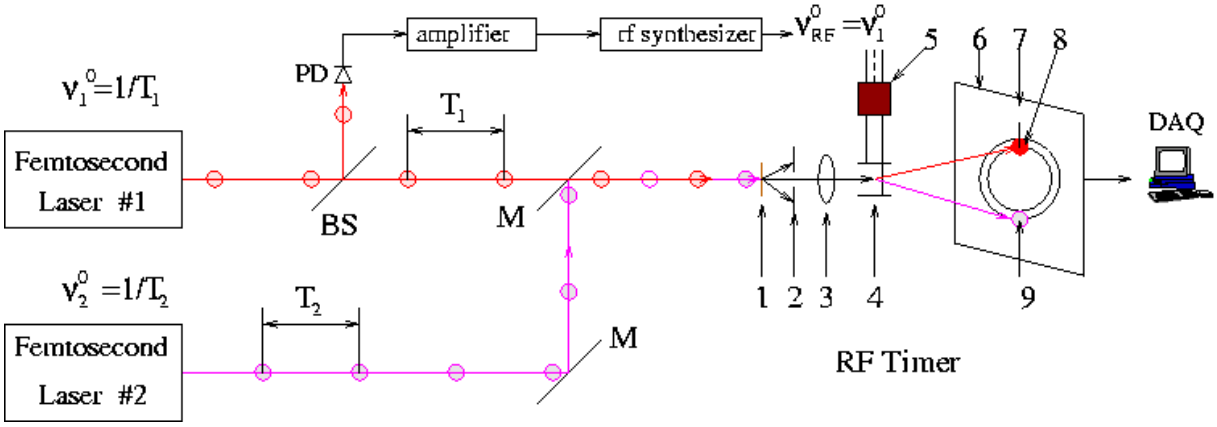

Fig. 5. Functional diagram of the optoelectronic heterodyne. BS – beam splitter, M – reflector, PD – photo diode, 1 – photocathode, 2 – accelerating electrode, 3 – electrostatic lens, 4 – deflection electrode, 5 – quarter wavelength coaxial cavity, 6 – position sensitive secondary electron detector, 7 – arbitrary reference fixed on SE detector readout system, 8 – and 9 – PE's from Laser #1 and Laser #2.

The two beam spots will drift with a repetition rate $\nu_H = \left|\nu_1^0 - \nu_2^0\right|$ and the long term instability of this $\Phi_2(t) - \Phi_1(t) \cong 2\pi(\nu_1^0 - \nu_2^0)$ beat signal is about 200 fs [5]. Therefore the optoelectronic heterodyning system based on the RF phototube and in conjunction with optical clocks can find

applications in ultra precise measurements, providing precisions comparable with precisions of optical clocks. The proposed technique is especially useful for measuring tiny beat frequency of two practically equal frequencies ν_1^0 and ν_2^0. In the case $\nu_1^0 = \nu_2^0$ the difference between frequencies can be determined with precision equal to

$$\nu_1^0 / \nu_2^0 - 1 = \sqrt{2} \times 200\, fs / \tau,$$

where τ is an averaging time interval. For $\tau = 10^5$ s, $\nu_1^0 / \nu_2^0 - 1$ can reach the value 3×10^{-18}, if the instabilities of femtosecond lasers are less than 3×10^{-18}.

3. Test of the Gravitational Red-shift

A typical gravitational red-shift experiment measures the frequency or wavelength shift $Z \equiv \Delta\nu / \nu$ between two identical frequency standards (clocks) placed at rest at different heights in a static gravitational field.

It can be shown (see, e.g., [8], p. 32) that the gravitational red-shift is a direct consequence of the Einstein Equivalence Principle (EEP). Under the assumption that the Weak Equivalence Principle (WEP) and Local Lorenz Invariance (LLI) are verified it can therefore be used to directly probe Local Position Invariance (LPI) by comparing two clocks that are at different positions and, in particular, at different gravitational potentials. A possible violation of LPI can then be simply modeled by allowing a composition and spatial dependence of the gravitational red-shift:

$$Z = (1 + \alpha^A) \frac{\Delta U}{c^2}.$$

The parameter α^A characterizes the violation of LPI for clocks of type A (e.g. Cs, H, Mg, cavity oscillators, optical clocks etc.), and $\frac{\Delta U}{c^2} \cong \frac{gH}{c^2} = H \times (1.09 \times 10^{-18})$ is the difference in Newtonian gravitational potential at the location of the two clocks, one of which is located at the Earth level and a similar one at the altitude H (in cm). Here g is the gravitational constant.

Limits on α can be obtained by either comparing two identical clocks at different potentials or by a null red-shift experiment, comparing non-identical co-located clocks A and B in a time-varying gravitational potential. The latter can be expressed as

$$\frac{\nu^A}{\nu^B} = \left(\frac{\nu^A}{\nu^B}\right)_0 \left(1 + \left(\alpha^A - \alpha^B\right) \frac{\Delta U}{c^2}\right),$$

where ν^A / ν^B is the locally measured frequency ratio and $\left(\nu^A / \nu^B\right)_0$ is that ratio at some initial location. Now ΔU is the variation of the Newtonian gravitational potential between that initial location and the current location of the clocks. The rates of two hydrogen maser clocks and of an ensemble of three superconducting-cavity stabilized oscillator (SCSO) clocks were compared over a

10 day period at Stanford University [9]. During this time, the solar gravitational potential changed sinusoidally with a 24 hour period by 3×10^{-13} because of the Earth's rotation, and changed linearly at 3×10^{-12} per day because the Earth is 90^{o} from perihelion in April. However, analysis of the data set an upper limit on both effects $\left|\alpha^{H}-\alpha^{SCSO}\right|<10^{-2}$. This bound has been improved using more stable frequency standards. The current bound, from comparing a Cesium atomic fountain with a Hydrogen maser for a year, is $\left|\alpha^{H}-\alpha^{Cs}\right|<2.1\times10^{-5}$ [10] (see also [11] and references therein).

Here we will consider the former case with two identical clocks in detail. The idea of using an atomic clock to test the gravitational red-shift was originated in the early 1950s by J.R. Zacharias [12], who in that time had pioneered the development of cesium atomic beam frequency standards. The concept was simple; place one clock on a mountain top, the other in a valley and transmit signals back and forth to compare their frequencies. However, in 1960, this work was eclipsed by the work of Pound, Rebka and Snyder [13, 14], who used the Mossbauer effect with γ rays from ^{57}Fe in a 75 ft. tower to obtain results confirming the gravitational red-shift prediction at the 1% level.

The concept of using clocks for testing the red-shift at a precision beyond 1% was revived in the post-Sputnik era of 1960, when the then newly developed hydrogen maser showed signs of achieving frequency stability in the 10^{-14} domain. The best current limit on α was obtained by the Gravity Probe-A (GP-A) experiment [15, 16]. In this experiment a rocket-borne H-maser was launched in a 10000 km near-vertical trajectory and tested Einstein's general theory of relativity. Interpreted as a limit on α, the experiment set $\left|\alpha\right|<7\times10^{-5}$.

The RF timing technique and optical clocks open new possibilities for high precision and Earth-bounded testing of gravitational red-shift. The experimental arrangement for identical clocks is shown schematically in Fig. 9. Two optical clocks are mounted with perpendicular axes. Both optical clocks are referenced to the same atomic transition and provide two OFCs with frequencies $\nu_1=1/T_1$ and $\nu_2=1/T_2$. For $H\cong200000$ cm, e.g. placing one clock on the Earth surface, another downstairs at SNOLAB [17], $\frac{\Delta U}{c^2}\cong H\times(1.09\times10^{-18})=2.18\times10^{-13}$, and $\nu_1=\nu_2-2.18\times10^{-13}$. This frequency difference will produce a beat signal with $\nu_1-\nu_2=2.18\times10^{-14}$ frequency of these two beam spots on the A and B RF timers. The beat signal will cause counterclockwise and clockwise drifts of beam spots relative to each other, on the scanning circles of the A and B RF timers, consequently. These drifts amount to 43.6 ns in a 10^5 s averaging time. As the proposed technique allows measurement of this drift with precision ~300 fs, the best current limit on α obtained by the GP-A experiment can be improved and set a limit $\left|\alpha\right|<0.7\times10^{-5}$ in an Earth-bounded experiment.

By using the RF phototube [4] instead of streak camera this limit can be decreased an order of magnitude and set a limit $|\alpha| < 0.7 \times 10^{-6}$. Consequently upper limit of the null red-shift experiments can be improved of about one-two orders of magnitude.

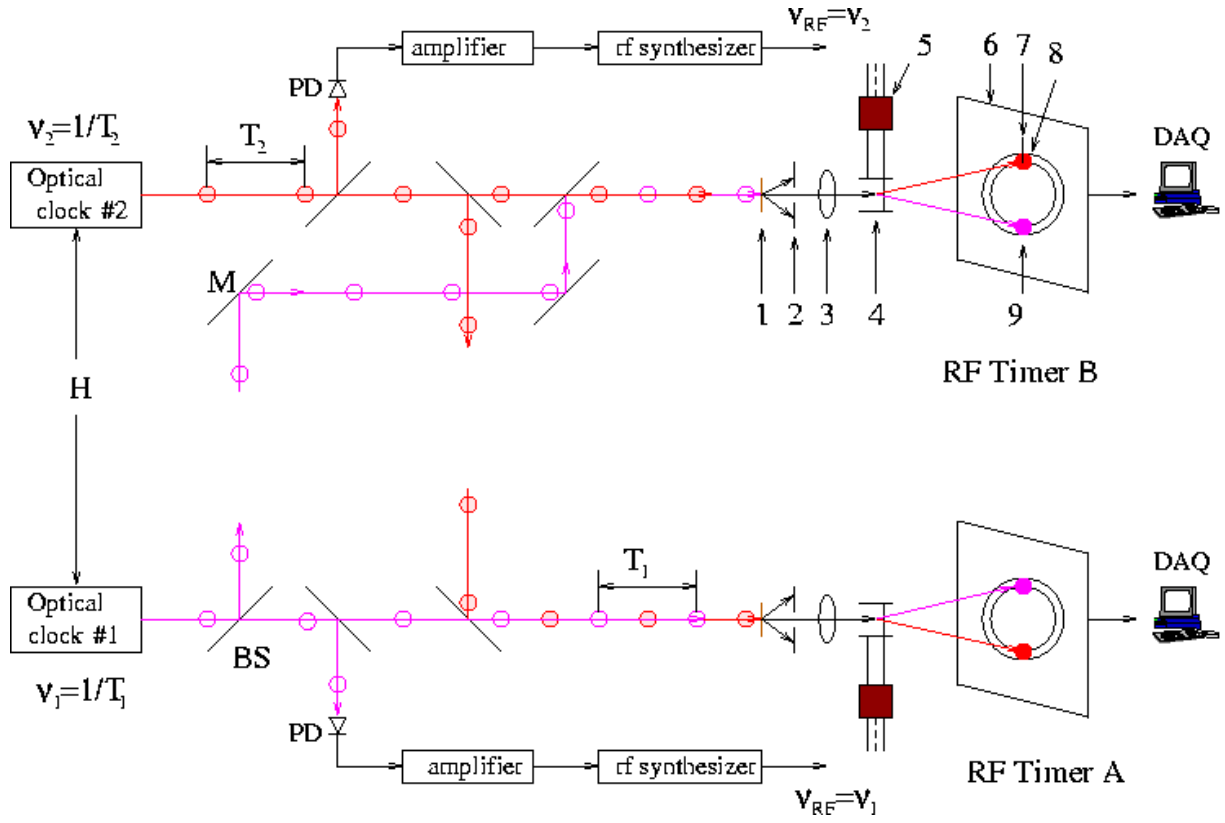

Fig. 9. Schematic of the gravitational red-shift experiment based on optoelectronic heterodyne. BS – beam splitter, M – reflector, PD – photo diode, 1 – photocathode, 2 – accelerating electrode, 3 – electrostatic lens, 4 – deflection electrode, 5 – quarter wavelength coaxial cavity, 6 – position sensitive secondary electron detector, 7 – arbitrary reference fixed on SE detector readout system, 8 and 9 – accelerated and deflected photoelectrons directly from #1 and #2 optical clocks.

4. Conclusions

A recently developed OFC in combination with a RF timing technique results in a highly stable (<300 fs in a day) optoelectronic heterodyne. Earth-bound gravitational red-shift precise experiments are the possible applications of the technique.

Acknowledgment

Author thanks Vahagn Gurzadyan and Mishik Kazaryan for useful discussions.

REFERENCES

1. S. A. Diddams, J. Ye, and L. Hollberg, “Femtosecond lasers for optical clocks and low noise frequency synthesis,” in *Femtosecond Optical Frequency Comb: Principle, Operation and Applications*, S. Cundiff and J. Ye, Eds. New York: Springer-Verlag (2004).
2. Th. Udem, R. Holzwarth, and Th. Haensch, Femtosecond optical frequency combs, Eur. Phys. J. Special Topics 172, 69 (2009).
3. T. M. Ramond, A. Bartels, S. A. Diddams, L. Hollberg, H. Kurz, Low Instability, Low Phase-Noise Femtosecond Optical Frequency Comb Microwave Synthesizer, Proceedings of the 2003 IEEE

International Frequency Control Symposium and PDA Exhibition Jointly with the 17th European Frequency and Time Forum, p. 168.
4. A. Margarayn, R. Carlini, R. Ent et al., Nucl. Instr. and Meth. A566, 321 (2006).
5. Wilfried Uhring, Chantal Virgine Zint, Patrick Summ, Bemard Cunin, Very high long-term stability synchroscan streak camera, Rev. Sci. Instrum. 74, 2646 (2003).
6. Claus Lammerzahl and Hansjorg Dittus, Time, Clocks and Fundamental Physics, Int. J. of Modern Phys. D, V. 16, 12B, 2455 (2007).
7. Samuel R. Stein, *Frequency and Time-Their Measurement and Characterization, Precision Frequency Control*, Vol. 2, edited by E.A. Gerber and A. Ballato (Academic Press, New York, 1985), pp. 191-416.
8. Clifford M. Will, *Theory and experiment in gravitational physics*, Cambridge University Press, 1992.
9. J. P. Turneaure et al., Test of the principle of equivalence by a null gravitational red-shift experiment, Phys. Rev. D, 27, 1705 (1983).
10. A. Godone, C. Novero, P. Tavella, Null gravitational red-shift experiment with nonidentical atomic clocks, Phys. Rev. D, 51, 319 (1995).
11. Clifford M. Will, The Confrontation between General Relativity and Experiment, arXiv:gr-qc/0510072 v2 4 April 2006.
12. J. R. Zacharias, Phys. Rev. 94 (1954) 751, see also in N. F. Ramsey, *Molecular Beams*, Oxford University Press, (1956) Chapter 9, paragraph 11.
13. R. V. Pound and G. A. Rebka, Apparent weight of photons, Phys. Rev. Lett. 4, 337 (1960).
14. R.V. Pound and J. L. Snider, Phys. Rev. Effect of gravity on gamma radiation, 140, B788 (1965).
15. Robert F. C. Vessot, "Past and future tests of relativistic gravitation with atomic clocks", The First William Fairbank Meeting on Relativistic Gravitational Experiments in Space, Editors: M. Demianski and C. W. F. Everitt, Advanced Series in Astrophysics and Cosmology-Vol. 7, p. 435, World Scientific, (1993).
16. R.F.C. Vessot et al., Test of relativistic gravitation with a space-borne hydrogen maser, Phys. Rev. Lett. 45, 2081 (1980).
17. http: //www.snolab.ca.